Convection and Magnetic Fields of Fast-Rotating Low-Mass Main Sequences Stars

Igor ROGACHEVSKII, Nathan KLEEORIN

Ben-Gurion University of the Negev, Beer Sheva

NORDITA, KTH Royal Institute of Technology and Stockholm University

Nikolay SAFIULLIN and Sergey PORSHNEV

Ural Federal University, Ekaterinburg

Roald GERSHBERG

Crimean Astrophysical Observatory

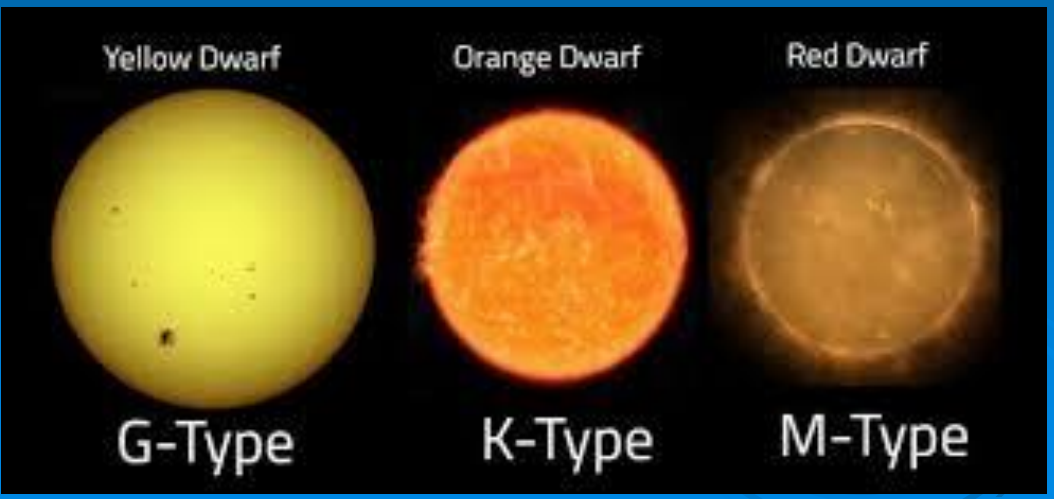

Fast-Rotating Low-Mass Main Sequences Stars

- The main sequences stars of the spectral class M composing 70 - 75 % of all star population, have: smaller sizes $(0.1\,R_\odot < R < 0.8\,R_\odot)$, masses $(0.08\,M_\odot < M < 0.55\,M_\odot)$ luminosity $(L \leq 0.05 L_\odot)$ in comparison with the Sun, and effective temperatures of $2500–4000\,K$ (Kochukhov 2021, Gershberg et al. 2024).

- About 15–20 per cent of these stars have similar magnetic activity as the Sun with cold magnetic spots and sporadic flares of very high releasing energy (Hawley et al. 2014 ; Newton et al. 2017).

- Fast rotating stars $(\Omega > 10\,\Omega_\odot)$ have strong poloidal magnetic fields at the pole, and sometimes they have strong toroidal magnetic fields at the pole (Strassmeier 2009; Morin et al. 2010).
- The periods of the stellar cycles can be in several times larger than the periods of the solar cycles (Bondar' et al. 2019).
- Magnetic fields of fast rotating stars can be more than several thousands Gauss (Kochukhov 2021).

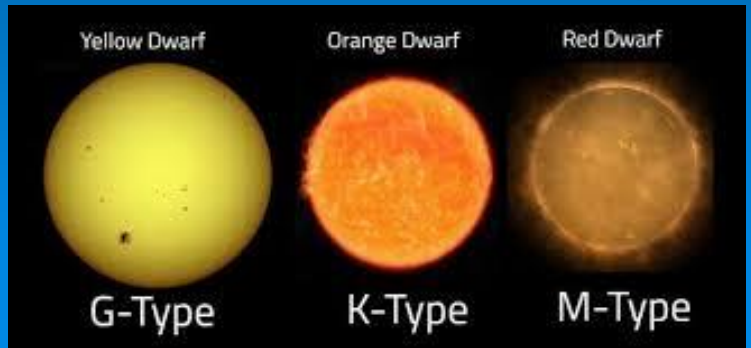

Monthly Notices
of the
ROYAL ASTRONOMICAL SOCIETY

MNRAS **526,** 1601–1612 (2023)
Advance Access publication 2023 September 27

https://doi.org/10.1093/mnras/stad2708

Magnetic fields of low-mass main sequences stars: non-linear dynamo theory and mean-field numerical simulations

N. Kleeorin,[1,2★] I. Rogachevskii,[1,3★] N. Safiullin,[2,4] R. Gershberg[5] and S. Porshnev[4,6]

ABSTRACT

Our theoretical and numerical analysis have suggested that for low-mass main sequences stars (of the spectral classes from M5 to G0) rotating much faster than the Sun, the generated large-scale magnetic field is caused by the mean-field $\alpha^2\Omega$ dynamo, whereby the α^2 dynamo is modified by a weak differential rotation. Even for a weak differential rotation, the behaviour of the magnetic activity is changed drastically from aperiodic regime to non-linear oscillations and appearance of a chaotic behaviour with increase of the differential rotation. Periods of the magnetic cycles decrease with increase of the differential rotation, and they vary from tens to thousand years. This long-term behaviour of the magnetic cycles may be related to the characteristic time of the evolution of the magnetic helicity density of the small-scale field. The performed analysis is based on the mean-field simulations (MFS) of the $\alpha^2\Omega$ and α^2 dynamos and a developed non-linear theory of α^2 dynamo. The applied MFS model was calibrated using turbulent parameters typical for the solar convective zone.

Modules for Experiments in Stellar Astrophysics (MESA)

- As a turbulent model of stellar convectiv e zones, we use ”Modules for Experiments in Stellar Astrophysics (MESA)” (Paxton et al. 2011).

- The MESA (http://mesa.sourceforge.net /) is one-dimensional stellar evolution module, which implements the standard mixing length theory (MLT) of convection (Cox and Giuli 1968).

- Using the MESA, we plot the radial profiles of
- the convective turbulent velocity,
- the turbulent magnetic diffusivity
- the Coriolis parameter
- for stars of late spectral classes: M6, M4, M2, K7, K4, K2, and G2. Here, H is the thickness of the convective zone, h is the height from the bottom of the convective zone.

Convective Turbulent Velocity

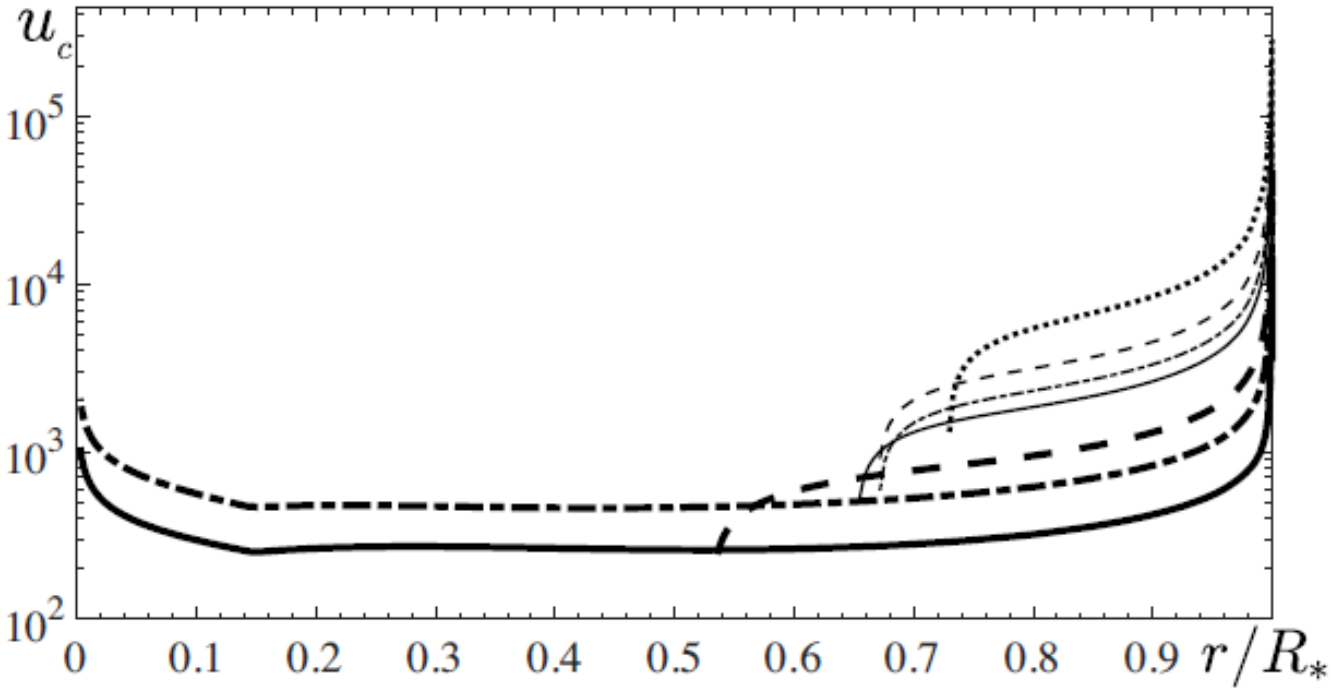

Figure 1. The radial profiles of the convective turbulent velocity u_c for the main sequences stars of the spectral classes: M6 (thick solid); M4 (thick dashed–dotted); M2 (thick dashed); K7 (thin solid); K4 (thin dashed-dotted); K2 (thin dashed); G2 (thin dotted). The velocity is measured in cm s^{-1}. Here, R_* is the star radius.

Turbulent Magnetic Diffusion

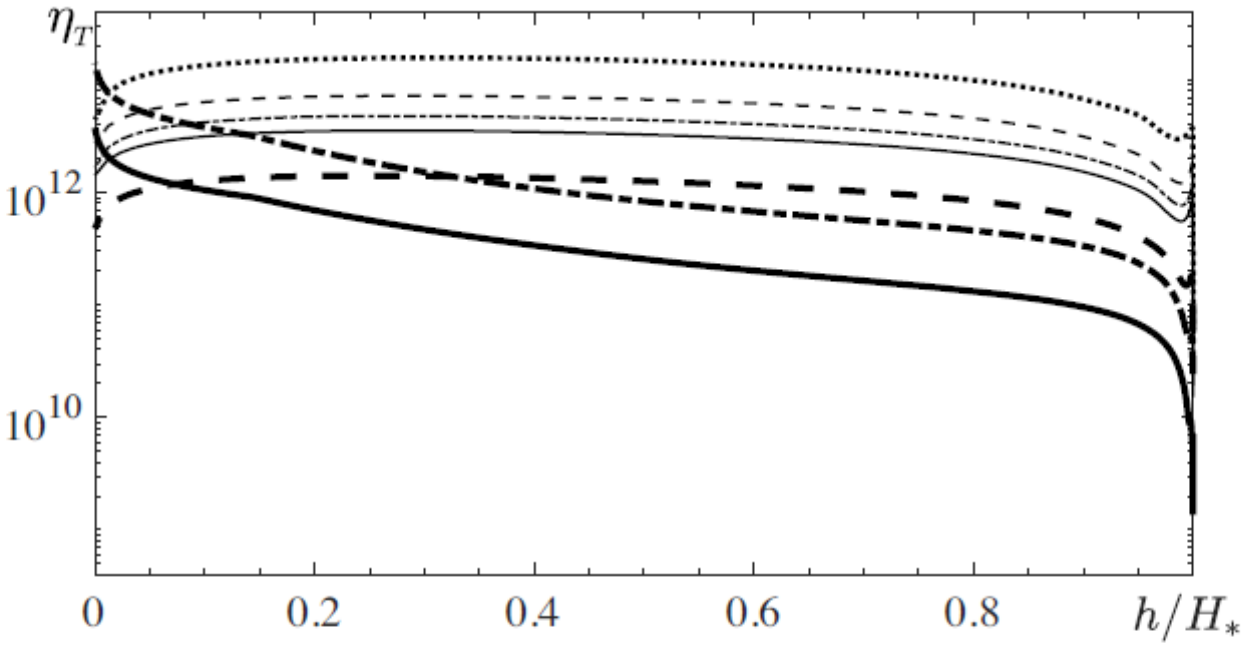

Figure 2. The radial profiles of the turbulent magnetic diffusivity η_T for the main sequences stars of the spectral classes: M6 (thick solid); M4 (thick dashed–dotted); M2 (thick dashed); K7 (thin solid); K4 (thin dashed–dotted); K2 (thin dashed); G2 (thin dotted). The turbulent magnetic diffusivity is measured in $\mathrm{cm}^2\ \mathrm{s}^{-1}$. Here, H_* is the thickness of the convective zone, and h is the height from the bottom of the convective zone.

Coriolis Parameter

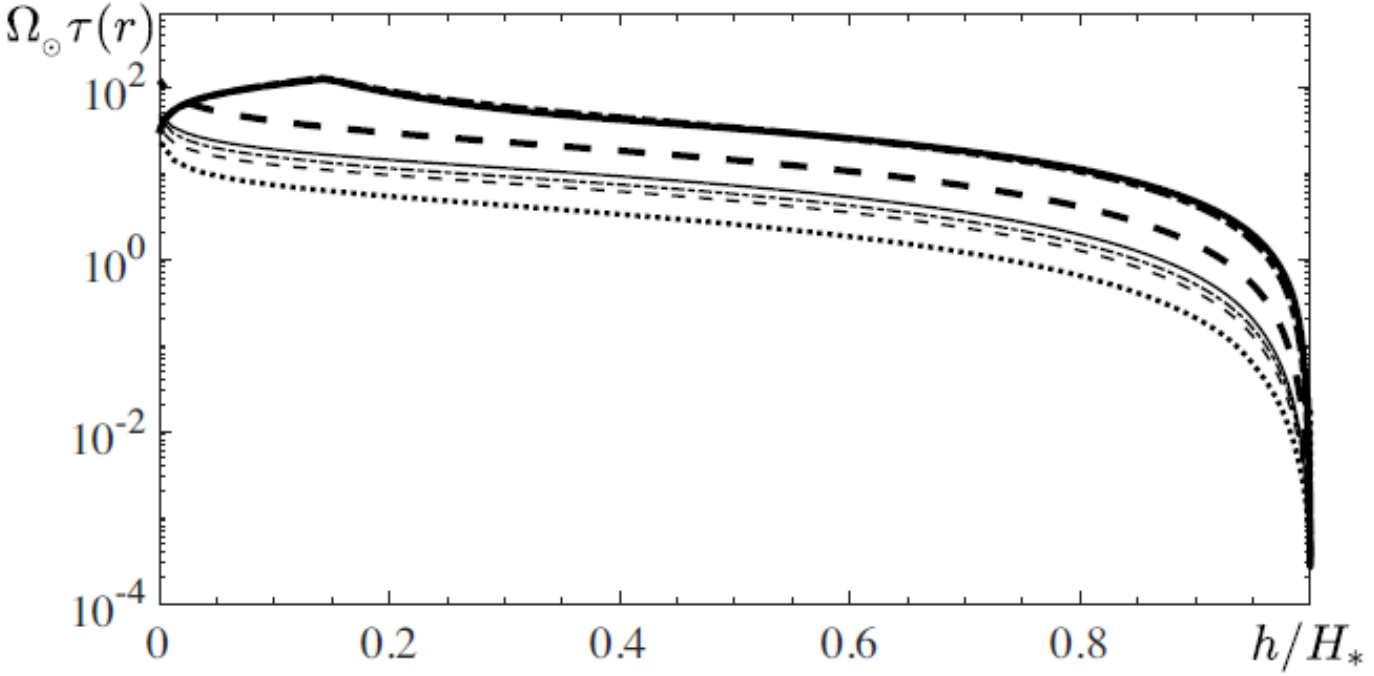

Figure 3. The radial profiles of the Coriolis parameter $\Omega_\odot \tau(h)$ based on the solar angular velocity $\Omega_\odot$ and the turbulent turn-over time $\tau(r) = 3\eta_T/u_c^2$ for the main sequences stars of the spectral classes: M6 (thick solid); M4 (thick dashed–dotted); M2 (thick dashed); K7 (thin solid); K4 (thin dashed–dotted); K2 (thin dashed); G2 (thin dotted). The turbulent magnetic diffusivity is measured in $\mathrm{cm}^2\,\mathrm{s}^{-1}$.

Mean-Field Dynamo

Mean-Field Approach: $\mathbf{H} = \mathbf{B} + \mathbf{b}, \quad \mathbf{V} = \mathbf{U} + \mathbf{u},$

- **Induction equation for mean magnetic field:**

$$\mathbf{B} = \langle \mathbf{H} \rangle, \qquad \mathbf{U} = \langle \mathbf{v} \rangle$$

$$\frac{\partial \mathbf{B}}{\partial t} = \nabla \times \left(\mathbf{U} \times \mathbf{B} + \boldsymbol{\varepsilon} - \eta \, \nabla \times \mathbf{B} \right)$$

- **Electromotive force:**

$$\boldsymbol{\varepsilon} \equiv \langle \mathbf{u} \times \mathbf{b} \rangle = \alpha \, \mathbf{B} - \eta_T \nabla \times \mathbf{B} + \ldots$$

$$\alpha = -\frac{\tau}{3} \langle \mathbf{u} \cdot \mathbf{rot}\, \mathbf{u} \rangle$$

Steenbeck, Krause, Rädler (1966)

Physics of the alpha-effect

Parker (1955); Steenbeck, Krause, Rädler (1966)

- The α - effect is related to the kinetic helicity in a density stratified convective turbulence.
- The deformations of the magnetic field lines are caused by upward and downward rotating turbulent eddies.
- The stratification of turbulence breaks a symmetry between the upward and downward eddies.
- Therefore, the total effect of the upward and downward eddies on the mean magnetic field does not vanish and it creates the mean electric current parallel to the original mean magnetic field.

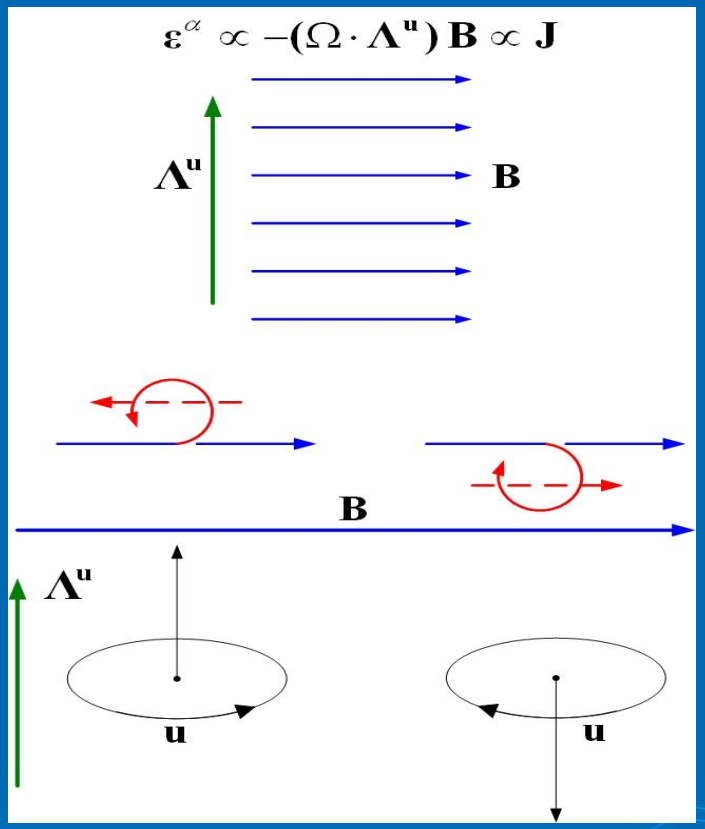

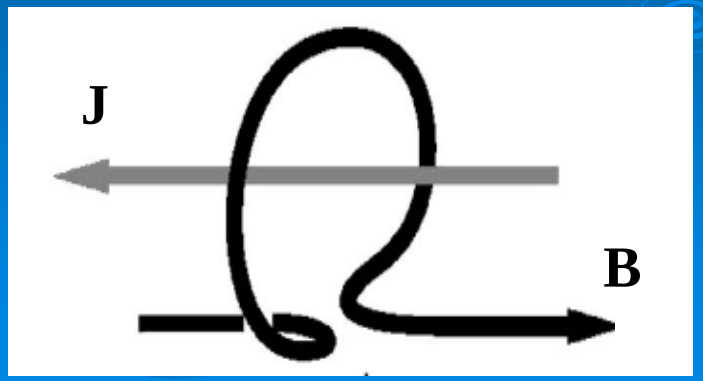

Profiles of Kinetic Alpha Effect

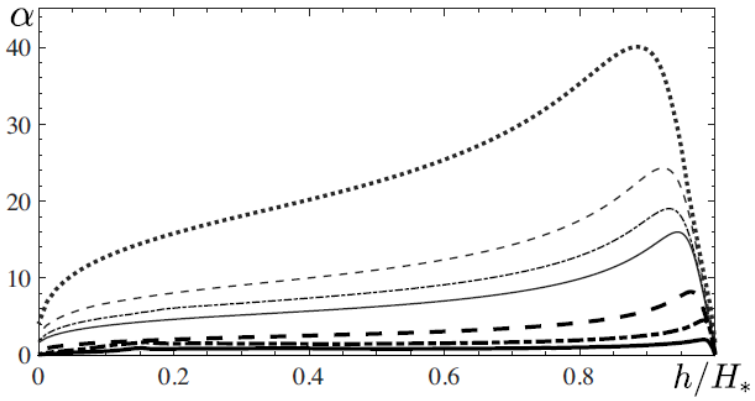

Figure 4. The radial profiles of the kinetic α-effect at the pole (at the latitude $\phi = \pi/2$) for isotropic turbulent convection for $\sigma = 1$ and $\varepsilon = 0$ for the main sequences stars of the spectral classes: M6 (thick solid); M4 (thick dashed–dotted); M2 (thick dashed); K7 (thin solid); K4 (thin dashed–dotted); K2 (thin dashed); G2 (thick dotted). The kinetic α is measured in m s^{-1}.

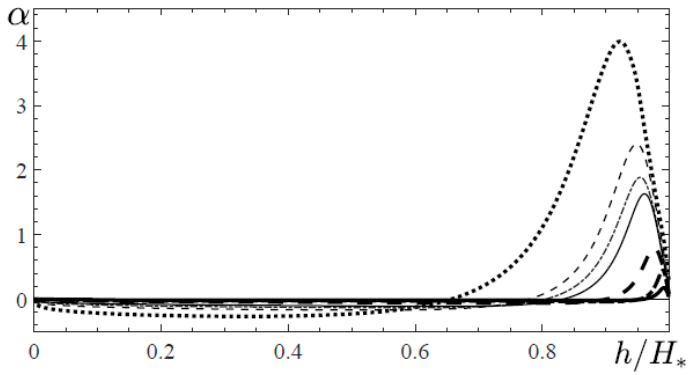

Figure 5. The radial profiles of the kinetic α effect at the latitude $\phi = \pi/6$ for anisotropic turbulent convection for $\sigma = 2$ and $\varepsilon = 1.2$ for the main sequences stars of the spectral classes: M6 (thick solid); M4 (thick dashed-dotted); M2 (thick dashed); K7 (thin solid); K4 (thin dashed-dotted); K2 (thin dashed); G2 (thick dotted). The kinetic α is measured in m/s.

Kleeorin and Rogachevskii, Phys. Rev. E , 67, 026321 (2003); JPP 84, 735840201 (2018)

$$\alpha = \frac{1}{6}\left(\frac{\ell_0^2\Omega}{H_\rho}\right)\sin\phi\,\left[\Psi_1(\omega) + \Psi_2(\omega)\sin^2\phi\right],$$

$\omega = 4\Omega\tau(r)$ for a slow rotation $(\omega \ll 1)$,

$$\alpha = \frac{4}{5}\left(\frac{\ell_0^2\Omega}{H_\rho}\right)\left(2 - \frac{\sigma}{3} - \frac{5\lambda}{6}\right)\sin\phi\ ,$$

the degree of anisotropy ε $\lambda = 2\varepsilon/(\varepsilon+2)$ $\varepsilon = \frac{2}{3}\left(\frac{\langle \mathbf{u}_\perp^2\rangle}{\langle \mathbf{u}_z^2\rangle} - 2\right)$,

The parameter σ determines the degree of thermal anisotropy

for fast rotation $(\omega \gg 1)$

$$\alpha = -\frac{\pi}{32}\left(\frac{\ell_0 u_c}{H_\rho}\right)\left(2\lambda + \frac{\sigma}{3} - 3 + (\sigma-1)\sin^2\phi\right)\sin\phi,$$

for $\sigma > 1$, the "pancake" thermal plumes

For $\sigma < 1$, the thermal plumes have the form of column or thermal jets

Thermal anisotropy: Plumes

For $\sigma < 1$,

$$\sigma = -3\left(\frac{3-4\left(\ell_{\rm h}^{\rm (pl)}/\ell_z^{\rm (pl)}\right)^{\frac{2}{3}}}{2+\left(\ell_{\rm h}^{\rm (pl)}/\ell_z^{\rm (pl)}\right)^{\frac{2}{3}}}\right)$$

for $\sigma > 1$, the "pancake" thermal plumes

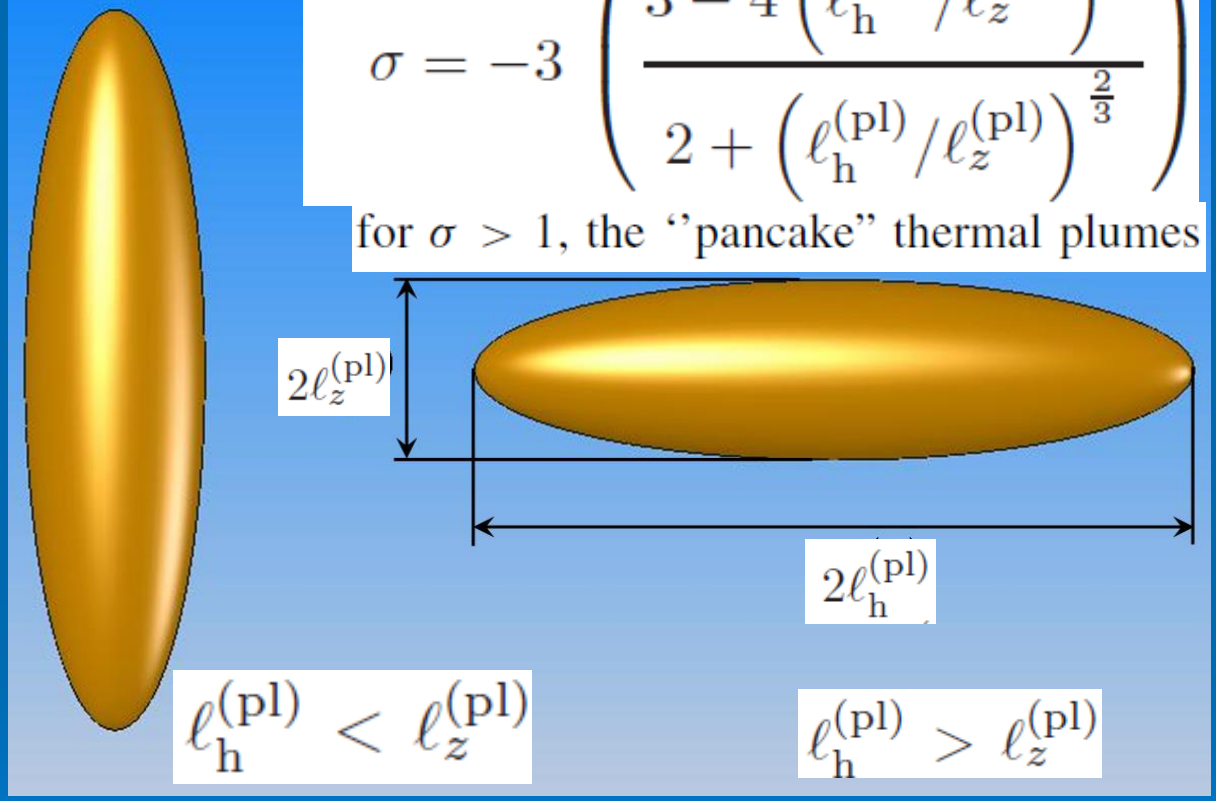

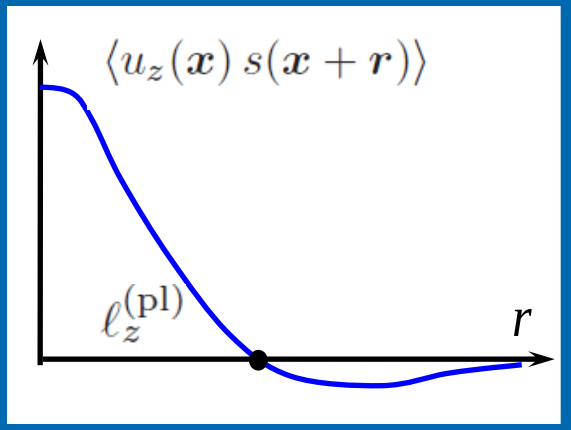

The parameter σ determines the degree of thermal anisotropy

"Column"-like plumes

"Pancake"-like plumes

$$F_z(\mathbf{k}) = \left(-\kappa_T \nabla_z \bar{\Theta}\right)\left[2\sigma - 3(\sigma-1)\left(\frac{k_\perp}{k}\right)^2\right]\frac{E(k)}{8\pi k^2}$$

Profiles of Kinetic Alpha Effect

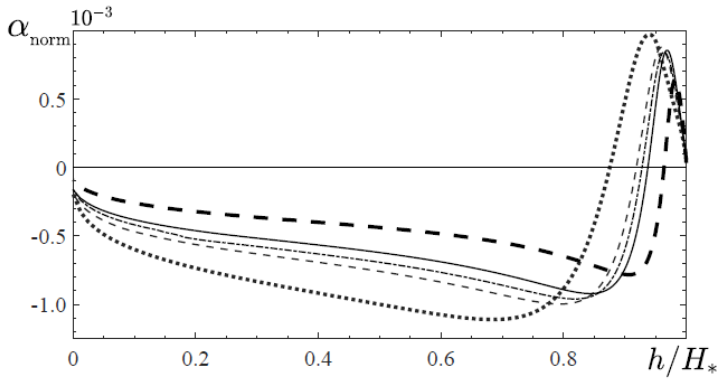

Figure 6. The radial profiles of the normalized kinetic α effect, $\alpha_{\rm norm} = \alpha/(\Omega_\odot\,\eta_T)^{1/2}$, at the latitude $\phi = \pi/6$ for $\sigma = 2$ and $\varepsilon = 1.2$, for the main sequences stars with the solar rotation rate of the spectral classes: M6 (thick solid); M4 (thick dashed-dotted); M2 (thick dashed); K7 (thin solid); K4 (thin dashed-dotted); K2 (thin dashed); G2 (thick dotted). Here H_* is the hight of the convective zone, and h is the hight from the bottom of the convective zone.

The maximum value of the kinetic α-effect can be estimated as (Kleeorin, Rogachevskii & Ruzmaikin 1995):

$$\alpha_* = C_*(\Omega_*\,\eta_{\rm T})^{1/2},$$

Table 1. The coefficient C_* for different spectral classes and different rotation rates.

spectral class	$\Omega_\odot$	$10\Omega_\odot$	$20\Omega_\odot$
G2	0.970	0.933	0.982
K2	0.877	0.874	0.883
K4	0.824	0.858	0.854
K7	0.855	0.815	0.793
M2	0.643	0.687	0.680

$$\alpha = \frac{1}{6}\left(\frac{\ell_0^2\Omega}{H_\rho}\right)\sin\phi\,\left[\Psi_1(\omega) + \Psi_2(\omega)\sin^2\phi\right],$$

$$\omega = 4\Omega\tau(r)$$

for a slow rotation $(\omega \ll 1)$,

$$\alpha = \frac{4}{5}\left(\frac{\ell_0^2\Omega}{H_\rho}\right)\left(2 - \frac{\sigma}{3} - \frac{5\lambda}{6}\right)\sin\phi\,,$$

the degree of anisotropy ε $\quad \lambda = 2\varepsilon/(\varepsilon+2)$ $\quad \varepsilon = \frac{2}{3}\left(\frac{\langle \mathbf{u}_\perp^2\rangle}{\langle \mathbf{u}_z^2\rangle} - 2\right),$

The parameter σ determines the degree of thermal anisotropy

for fast rotation $(\omega \gg 1)$

$$\alpha = -\frac{\pi}{32}\left(\frac{\ell_0 u_c}{H_\rho}\right)\left(2\lambda + \frac{\sigma}{3} - 3 + (\sigma-1)\sin^2\phi\right)\sin\phi,$$

for $\sigma > 1$, the "pancake" thermal plumes

For $\sigma < 1$, the thermal plumes have the form of column or thermal jets

Profiles of Kinetic Alpha Effect

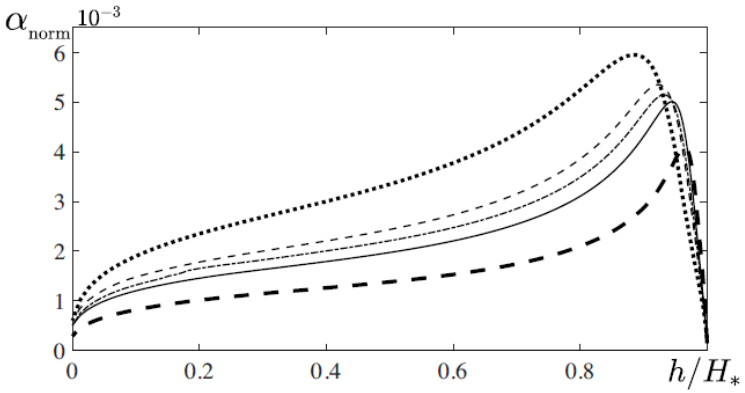

Figure 7. The radial profiles of the normalized kinetic α-effect, $\alpha_{\rm norm} = \alpha/(10\Omega_\odot\,\eta_{\rm T})^{1/2}$, at the pole ($\phi = \pi/2$) for $\sigma = 1$ and $\varepsilon = 0$, for the main sequences stars of the spectral classes: M6 (thick solid); M4 (thick dashed–dotted); M2 (thick dashed); K7 (thin solid); K4 (thin dashed–dotted); K2 (thin dashed); G2 (thick dotted). Here, H_* is the height of the convective zone, and h is the height from the bottom of the convective zone.

The maximum value of the kinetic α-effect can be estimated as (Kleeorin, Rogachevskii & Ruzmaikin 1995):

$$\alpha_* = C_*(\Omega_*\,\eta_{\rm T})^{1/2},$$

Table 1. The coefficient C_* for different spectral classes and different rotation rates.

spectral class	$\Omega_\odot$	$10\Omega_\odot$	$20\Omega_\odot$
G2	0.970	0.933	0.982
K2	0.877	0.874	0.883
K4	0.824	0.858	0.854
K7	0.855	0.815	0.793
M2	0.643	0.687	0.680

$$\alpha = \frac{1}{6}\left(\frac{\ell_0^2\Omega}{H_\rho}\right)\sin\phi\,\left[\Psi_1(\omega) + \Psi_2(\omega)\sin^2\phi\right],$$

$\omega = 4\Omega\tau(r)$ for a slow rotation ($\omega \ll 1$),

$$\alpha = \frac{4}{5}\left(\frac{\ell_0^2\Omega}{H_\rho}\right)\left(2 - \frac{\sigma}{3} - \frac{5\lambda}{6}\right)\sin\phi\,,$$

the degree of anisotropy ε $\lambda = 2\varepsilon/(\varepsilon+2)$ $\varepsilon = \frac{2}{3}\left(\frac{\langle \mathbf{u}_\perp^2\rangle}{\langle \mathbf{u}_z^2\rangle} - 2\right)$,

The parameter σ determines the degree of thermal anisotropy

for fast rotation ($\omega \gg 1$)

$$\alpha = -\frac{\pi}{32}\left(\frac{\ell_0 u_c}{H_\rho}\right)\left(2\lambda + \frac{\sigma}{3} - 3 + (\sigma-1)\sin^2\phi\right)\sin\phi,$$

for $\sigma > 1$, the ''pancake'' thermal plumes

For $\sigma < 1$, the thermal plumes have the form of column or thermal jets

Estimate for Kinetic Alpha Effect

The maximum value of the kinetic α-effect can be estimated as (Kleeorin, Rogachevskii & Ruzmaikin 1995):

$$\alpha_* = C_* (\Omega_* \eta_T)^{1/2},$$

$$\alpha \simeq \ell(r)\Omega_* \text{ for } \ell(r)\Omega_*/u_c(r) \ll 1,$$

$$\alpha \simeq u_c(r) \text{ for } \ell(r)\Omega_*/u_c(r) \gg 1$$

Table 1. The coefficient C_* for different spectral classes and different rotation rates.

spectral class	$\Omega_\odot$	$10\Omega_\odot$	$20\Omega_\odot$
G2	0.970	0.933	0.982
K2	0.877	0.874	0.883
K4	0.824	0.858	0.854
K7	0.855	0.815	0.793
M2	0.643	0.687	0.680

for a slow rotation ($\omega \ll 1$),

$$\alpha = \frac{4}{5}\left(\frac{\ell_0^2 \Omega}{H_\rho}\right)\left(2 - \frac{\sigma}{3} - \frac{5\lambda}{6}\right)\sin\phi\ ,$$

for fast rotation ($\omega \gg 1$)

$$\alpha = -\frac{\pi}{32}\left(\frac{\ell_0 u_c}{H_\rho}\right)\left(2\lambda + \frac{\sigma}{3} - 3 + (\sigma - 1)\sin^2\phi\right)\sin\phi,$$

The kinetic alpha effect reaches a maximum at the depth determined by the condition:

$$\ell_m(r_m) = u_c(r_m)/\Omega_*.$$

$$\ell_m(r_m) \simeq (\eta_T/\Omega_*)^{1/2}$$

$$\eta_T \simeq \ell_m(r_m) u_c(r_m)$$

The maximal value of the kinetic alpha effect is estimated as

$$\alpha_* \simeq u_c(r_m) \simeq \eta_T/\ell_m(r_m) \simeq (\eta_T \Omega_*)^{1/2}.$$

Differential Rotation

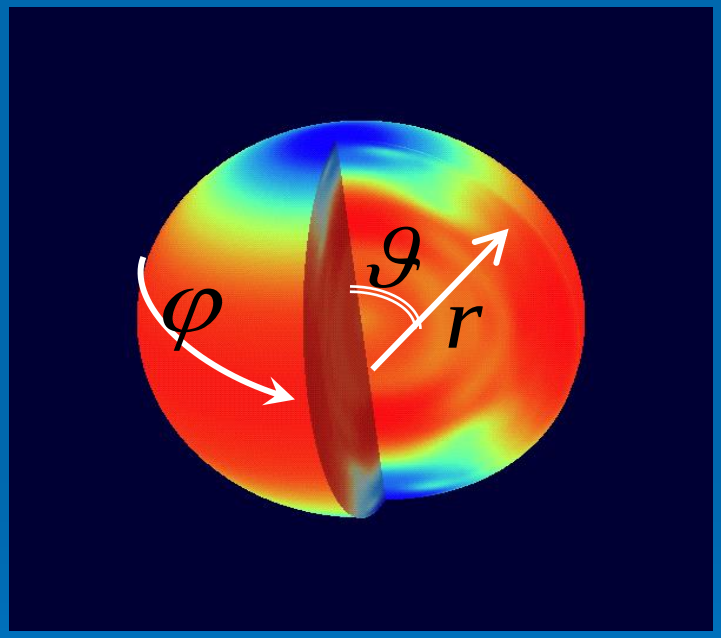

Kosovichev et al. (1997)

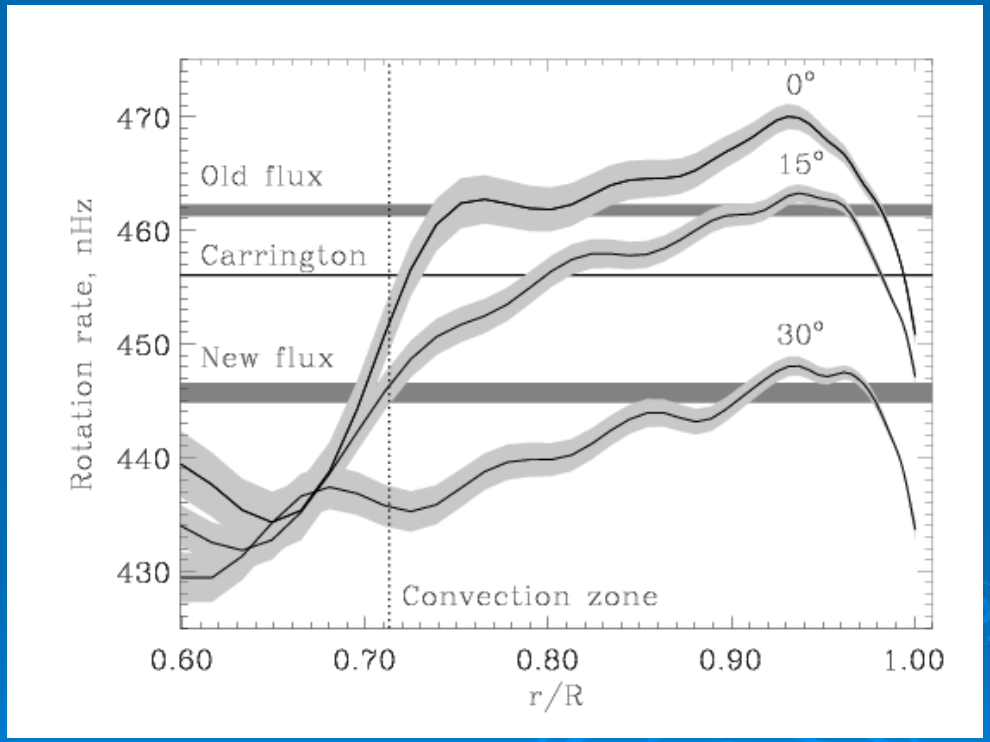

Theory of Differential Rotation

Rogachevskii and Kleeorin (2018), J. Plasma Phys., 84, 735840201
Kleeorin and Rogachevskii (2006), Phys. Rev. E , 73, 046303

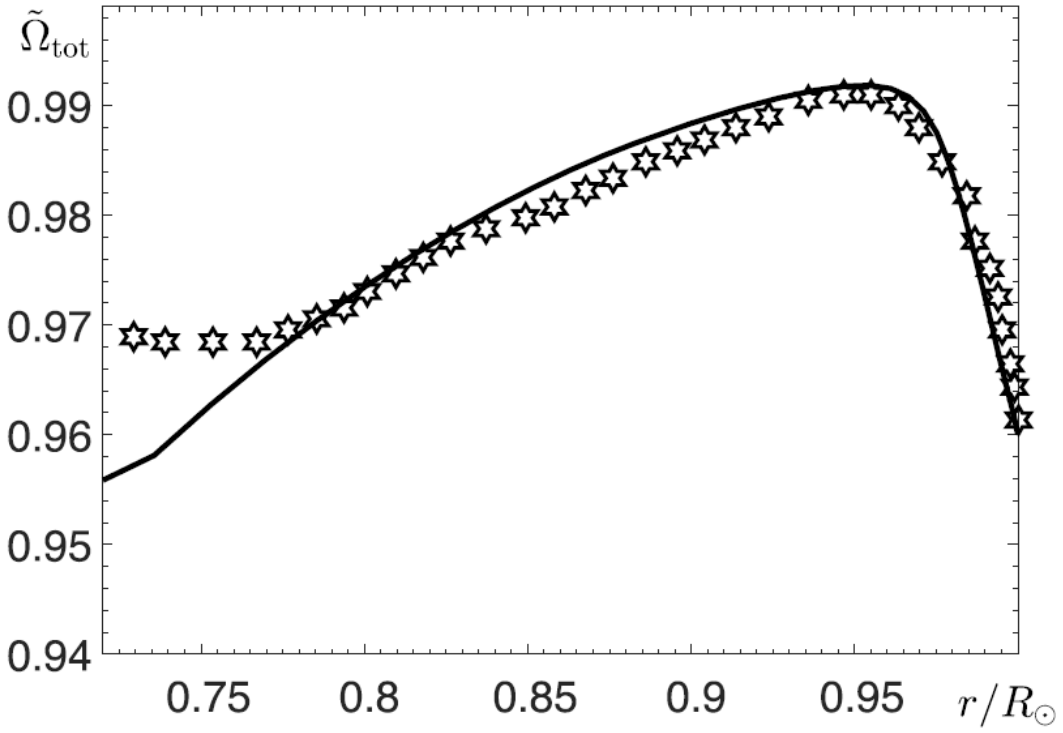

FIGURE 2. The total angular velocity $\tilde{\Omega}_{tot} = \tilde{\Omega}_0 + 1$ that includes the uniform rotation Ω versus the radius $r/R_\odot$ (solid). This theoretical profile is compared with the radial profile of the solar angular velocity obtained from helioseismology observational data (stars) at the latitude $\phi = 30°$ and normalized by the solar rotation frequency $\Omega_\odot(\phi = 0)$ at the equator, where $R_\odot$ is the solar radius.

Generation of the mean magnetic field due to the dynamo

Mean magnetic field:

$$\mathbf{B} = B_\varphi\, \mathbf{e}_\varphi + \nabla \times [A\, \mathbf{e}_\varphi]$$

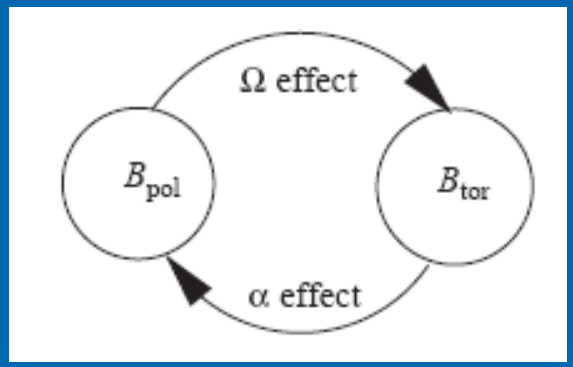

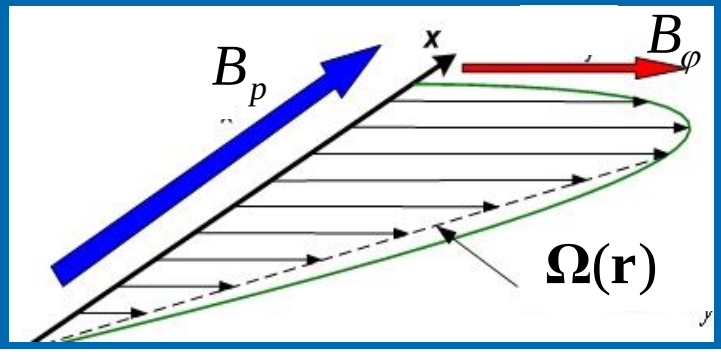

$$\int_{r_c}^{1} (\partial^2 \overline{B}_\varphi / \partial r^2)\, \mathrm{d}r = -(\mu^2/3)\overline{B}_\varphi .$$

$$\frac{\partial \overline{B}_\varphi}{\partial t} = \left[R_\alpha R_\omega \sin\theta \frac{\partial}{\partial \theta} - R_\alpha^2 \left(\frac{\partial^2}{\partial \theta^2} - \mu^2 \right) \right] \overline{A} + \left(\frac{\partial^2}{\partial \theta^2} - \mu^2 \right) \overline{B}_\varphi ,$$

$$\frac{\partial \overline{A}}{\partial t} = \alpha \overline{B}_\varphi + \left(\frac{\partial^2}{\partial \theta^2} - \mu^2 \right) \overline{A}.$$

Dynamo number:

$$R_\alpha = \alpha_* R_* / \eta_T \qquad R_\omega = (\delta\Omega)\, R_*^2 / \eta_T .$$

Kinematic $\alpha^2\,\Omega$ dynamo

$$\frac{\partial \overline{B}_\varphi}{\partial t} = \left[R_\alpha\, R_\omega\, \sin\theta \frac{\partial}{\partial \theta} - R_\alpha^2 \left(\frac{\partial^2}{\partial \theta^2} - \mu^2\right)\right] \overline{A} + \left(\frac{\partial^2}{\partial \theta^2} - \mu^2\right) \overline{B}_\varphi,$$

$$\frac{\partial \overline{A}}{\partial t} = \alpha \overline{B}_\varphi + \left(\frac{\partial^2}{\partial \theta^2} - \mu^2\right) \overline{A}.$$

$$\gamma = \frac{R_\alpha R_\alpha^{\rm cr}}{\sqrt{2}} \left[\left[1 + \left(\frac{\zeta R_\omega}{R_\alpha R_\alpha^{\rm cr}}\right)^2\right]^{1/2} + 1\right]^{1/2} - \left(R_\alpha^{\rm cr}\right)^2,$$

$$\omega = -{\rm sgn}(R_\omega) \frac{R_\alpha R_\alpha^{\rm cr}}{\sqrt{2}} \left[\left[1 + \left(\frac{\zeta R_\omega}{R_\alpha R_\alpha^{\rm cr}}\right)^2\right]^{1/2} - 1\right]^{1/2},$$

$$\int_{r_c}^{1} (\partial^2 \overline{B}_\varphi / \partial r^2)\, {\rm d}r = -(\mu^2/3) \overline{B}_\varphi.$$

$$\frac{\overline{B}_{\rm pol}^2}{\overline{B}_\varphi^2} = \left[1 + \left(\frac{\zeta R_\omega}{R_\alpha R_\alpha^{\rm cr}}\right)^2\right]^{-1/2}$$

for a weak differential rotation,

$$\zeta R_\omega \ll R_\alpha R_\alpha^{\rm cr}$$

$$\zeta^2 = 1 - \left(\mu / R_\alpha^{\rm cr}\right)^2$$

$$\gamma = R_\alpha R_\alpha^{\rm cr} \left[1 + \frac{1}{8}\left(\frac{\zeta R_\omega}{R_\alpha R_\alpha^{\rm cr}}\right)^2\right] - \left(R_\alpha^{\rm cr}\right)^2,$$

$$\omega = -\frac{\zeta R_\omega}{\sqrt{2}}.$$

$$R_\alpha = \alpha_* R_* / \eta_T$$

$$R_\omega = (\delta\Omega)\, R_*^2 / \eta_T.$$

$$\overline{B}^2 = \overline{B}_\varphi^2 + R_\alpha^2 \left[\mu^2 \overline{A}^2 + \left(\frac{\partial \overline{A}}{\partial \theta}\right)^2\right].$$

$$T_{\rm dyn} = (2\pi/\omega)\,(R_*^2/\eta_{\rm T}).$$

Algebraic and Dynamic Nonlinearities in Mean-Field Dynamo

- **Induction equation for mean magnetic field:**

$$\frac{\partial \mathbf{B}}{\partial t} = \boldsymbol{\nabla} \times (\mathbf{U} \times \mathbf{B} + \boldsymbol{\mathcal{E}} - \eta \boldsymbol{\nabla} \times \mathbf{B}),$$

- **Nonlinear electromotive force:** $\boldsymbol{\mathcal{E}}(\mathbf{B}) = \langle \mathbf{u} \times \mathbf{b} \rangle$

$$\boldsymbol{\mathcal{E}}(\mathbf{B}) = \alpha(\mathbf{B})\,\mathbf{B} - [\mathbf{V}^A(B)\cdot\boldsymbol{\nabla}]\,\mathbf{A} - \eta_T^{A,B}(B)\,(\boldsymbol{\nabla}\times\mathbf{B})$$

- **Total (kinetic + magnetic) nonlinear alpha effect :**

$$\alpha(\mathbf{B}) = \alpha^v + \alpha^m = \chi^v\,\Phi_v(B) + \chi^c(\mathbf{B})\,\Phi_m(B)$$

$$\chi^c(\mathbf{B}) = \frac{\tau}{3\rho}\langle \mathbf{b}\cdot(\nabla\times\mathbf{b})\rangle = \frac{2}{9\eta_T\rho}\langle \mathbf{a}\cdot\mathbf{b}\rangle + O\Big(\frac{l_0^2}{L_u^2}\Big)$$

Methods for Derivation of EMF

- **Quasi-Linear Approach** or Second-Order Correlation Approximation (SOCA) or First-Order Smoothing Approximation (FOSA)

  Rm << 1 , Re << 1

  Steenbeck, Krause, Rädler (1966); Roberts, Soward (1975); Moffatt (1978)

- **Path-Integral Approach** (delta-correlated in time random velocity field or short yet finite correlation time)

  Zeldovich, Molchanov, Ruzmaikin, Sokoloff (1988)

  Rogachevskii, Kleeorin (1997)

  $$\mathrm{St} = \frac{\tau}{\ell/u} \ll 1$$

- **Tau-approaches** (spectral tau-approximation, minimal tau-approximation) – **third-order or high-order closure**

  Re >> 1 and Rm >> 1

  Pouquet, Frisch, Leorat (1976);

  Rogachevskii, Kleeorin (2000; 2001; 2003); Blackman, Field (2002);

  Rädler, Kleeorin, Rogachevskii (2003)

- **Renormalization Procedure** (renormalization of viscosity, diffusion, electromotive force and other turbulent transport coefficients) - **there is no separation of scales**

  Moffatt (1981; 1983); Kleeorin, Rogachevskii (1994)

I. Rogachevskii, “Introduction to Turbulent Transport of Particles, Temperature and Magnetic Fields” (Cambridge University Press, Cambridge, 2021).

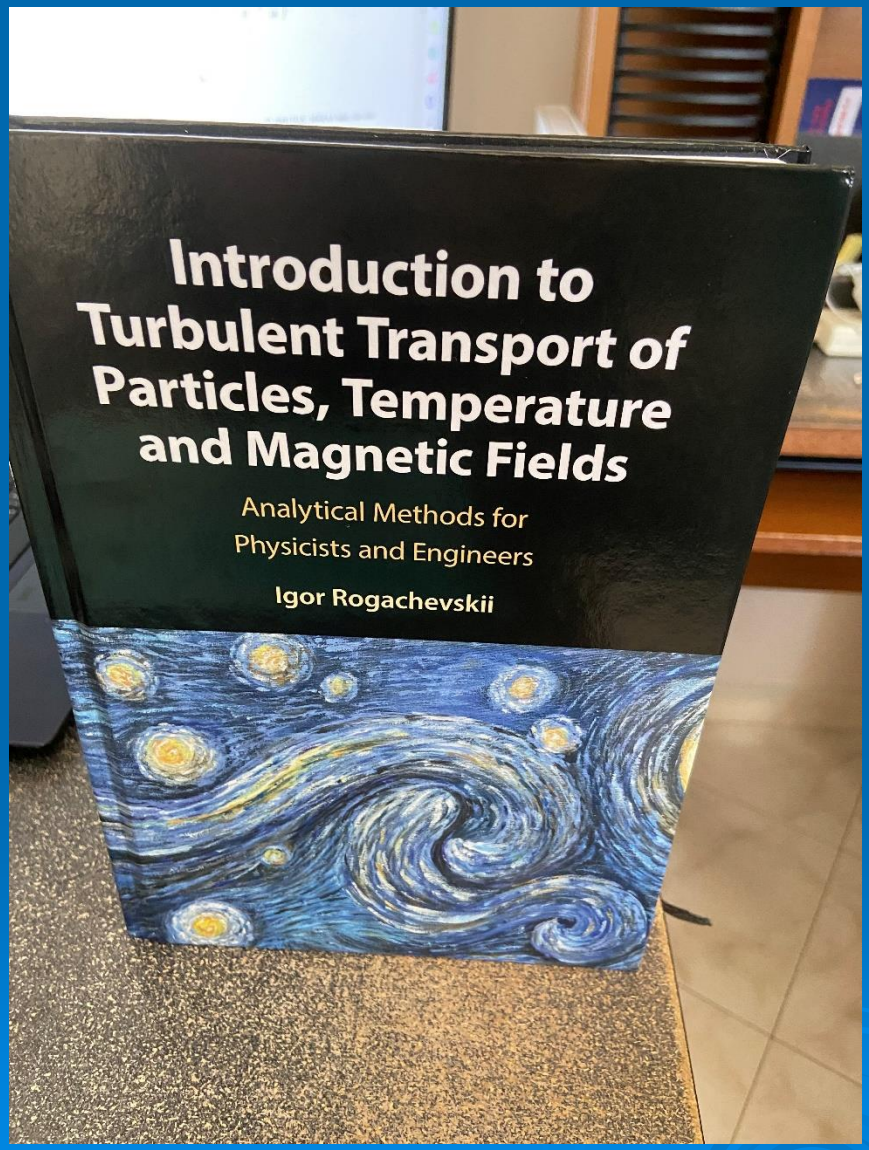

- Various analytical methods are applied in this book:
- Mean-field approach;
- Multi-scale approach;
- Dimensional analysis;
- Quasi-linear approach;
- Tau approach;
- Path-integral approach;
- Analyses based on the budget equations.
- One-way and two-way couplings between turbulence and particles, or temperature, or magnetic fields are described.

- Table of Contents:

Nonlinear Effect: Magnetic Part of Alpha effect

- **Induction equation for mean magnetic field:**

$$\frac{\partial \mathbf{B}}{\partial t} = \nabla \times \left(\mathbf{U} \times \mathbf{B} + \boldsymbol{\varepsilon} - \eta \ \nabla \times \mathbf{B} \right)$$

- **Electromotive force:**

$$\boldsymbol{\varepsilon} \equiv \left\langle \mathbf{u} \times \mathbf{b} \right\rangle = \alpha \mathbf{B} - \eta_T \nabla \times \mathbf{B} + \ldots$$

$$\alpha = -\frac{\tau}{3} \left\langle \mathbf{u} \cdot \mathbf{rot}\ \mathbf{u} \right\rangle + \frac{\tau}{12\pi\rho} \underbrace{\left\langle \mathbf{b} \cdot \mathbf{rot}\ \mathbf{b} \right\rangle}_{\sim \mathbf{a} \cdot \mathbf{b}}$$

A. Pouquet, U. Frisch, and J. Leorat, J. Fluid Mech. 77, 321 (1976)

Magnetic Helicity

Total magnetic helicity is conserved for very large magnetic Reynolds numbers

$$\chi^m_{\text{total}}(\mathbf{B}) = \mathbf{A}\cdot\mathbf{B} + \langle \mathbf{a}\cdot\mathbf{b}\rangle \to const$$

Magnetic part of alpha effect:

$$\alpha^m = \chi^c(\mathbf{B})\,\Phi_m(B)$$

The dynamic nonlinearity:

$$\chi^c(\mathbf{B}) \sim \frac{2}{9\eta_T\rho}\langle \mathbf{a}\cdot\mathbf{b}\rangle$$

The evolutionary equation: $\chi^{(m)}(\mathbf{B}) = \langle \mathbf{a}\cdot\mathbf{b}\rangle$

$$\frac{\partial \chi^c}{\partial t} + \frac{\chi^c}{\tau\,\mathrm{Rm}} + \nabla\cdot\mathbf{F} = -\frac{4}{9\eta_T\rho}\boldsymbol{\mathcal{E}}\cdot\mathbf{B}$$

Dynamic nonlinearity

$$\frac{\partial \chi^c}{\partial t} + \frac{\chi^c}{\tau\,\mathrm{Rm}} + \nabla \cdot \mathbf{F} = -\frac{4}{9\eta_T \rho}\,\boldsymbol{\mathcal{E}} \cdot \mathbf{B}$$

Kleeorin and Ruzmaikin (1982) – for isotropic turbulence
Kleeorin and Rogachevskii (1999) – for anisotropic turbulence

In the absence of the magnetic helicity fluxes $\longrightarrow$ catastrophic quenching

$$\alpha = \frac{\alpha_v}{1 + Rm\, B^2/B_{\rm eq}^2}$$

Vainshtein and Cattaneo (1992);
Gruzinov and Diamond (1994)

Open Boundary Conditions $\longrightarrow$ Effect of Magnetic Helicity Fluxes

Blackman and Field (2000); Kleeorin, Moss, Rogachevskii and Sokoloff (2000);

$$\alpha = -\frac{\tau\,\mathrm{div}\,\mathbf{F}}{B^2/B_{\rm eq}^2}$$

Different Forms of Magnetic Helicity Fluxes:
Kleeorin and Rogachevskii (1999); Kleeorin, Moss, Rogachevskii and Sokoloff (2000, 2002, 2003), Vishniac and Cho (2001); Brandenburg and Subramanian (2005) – review,
Kleeorin and Rogachevskii (2022), Gopalakrishnan and Subramanian (2023)

Generation of the mean magnetic field due to the dynamo

Mean magnetic field:

$$\mathbf{B} = B_\varphi\, \mathbf{e}_\varphi + \nabla \times [A\, \mathbf{e}_\varphi]$$

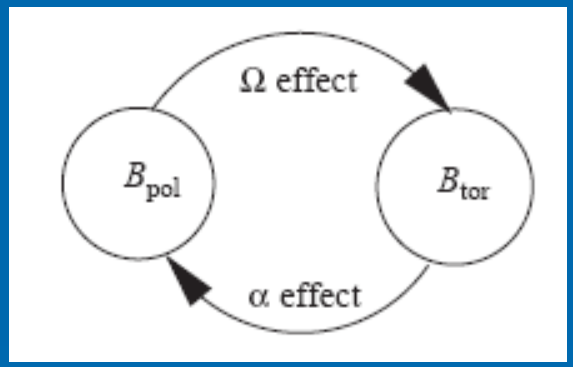

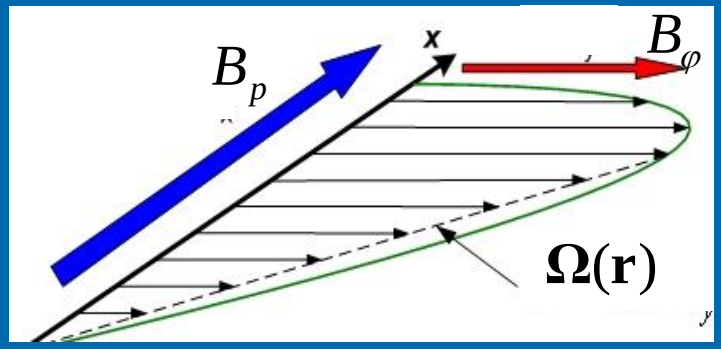

$$\int_{r_c}^{1} (\partial^2 \overline{B}_\varphi / \partial r^2)\, \mathrm{d}r = -(\mu^2/3)\overline{B}_\varphi .$$

$$\frac{\partial \overline{B}_\varphi}{\partial t} = \left[R_\alpha R_\omega \sin\theta \frac{\partial}{\partial \theta} - R_\alpha^2 \left(\frac{\partial^2}{\partial \theta^2} - \mu^2 \right) \right] \overline{A} + \left(\frac{\partial^2}{\partial \theta^2} - \mu^2 \right) \overline{B}_\varphi ,$$

$$\frac{\partial \overline{A}}{\partial t} = \alpha \overline{B}_\varphi + \left(\frac{\partial^2}{\partial \theta^2} - \mu^2 \right) \overline{A}.$$

Dynamo number:

$$R_\alpha = \alpha_* R_* / \eta_T \qquad R_\omega = (\delta\Omega)\, R_*^2 / \eta_T .$$

Magnetic Helicity

Total magnetic helicity is conserved for very large magnetic Reynolds numbers

$$\chi^m_{\text{total}}(\mathbf{B}) = \mathbf{A}\cdot\mathbf{B} + \langle \mathbf{a}\cdot\mathbf{b}\rangle \to const$$

Magnetic part of alpha effect:

$$\alpha^m = \chi^c(\mathbf{B})\,\Phi_m(B)$$

The dynamic nonlinearity:

$$\chi^c(\mathbf{B}) \sim \frac{2}{9\eta_T\rho}\langle \mathbf{a}\cdot\mathbf{b}\rangle$$

The evolutionary equation: $\chi^{(m)}(\mathbf{B}) = \langle \mathbf{a}\cdot\mathbf{b}\rangle$

$$\frac{\partial \chi^c}{\partial t} + \frac{\chi^c}{\tau\,\mathrm{Rm}} + \nabla\cdot\mathbf{F} = -\frac{4}{9\eta_T\rho}\boldsymbol{\mathcal{E}}\cdot\mathbf{B}$$

$\alpha^2\,\Omega$ dynamo

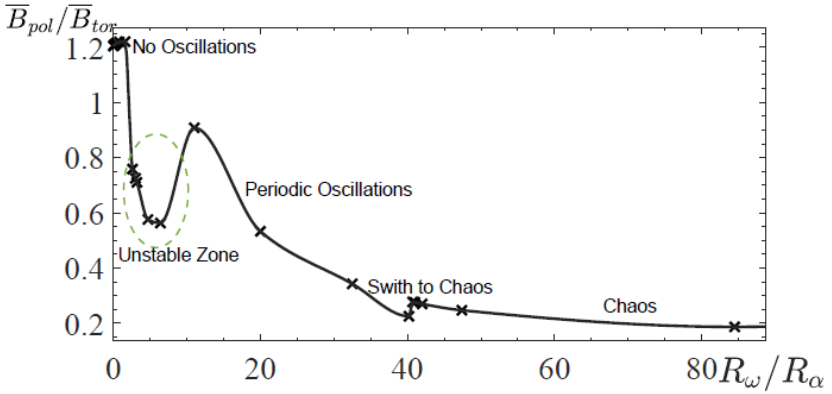

Figure 8. The ratio of the maximum values of the poloidal to toroidal mean magnetic fields $\overline{B}_{\rm pol}/\overline{B}_{\rm tor}$ versus R_ω/R_α obtained from numerical simulations of $\alpha^2\Omega$ mean-field dynamo.

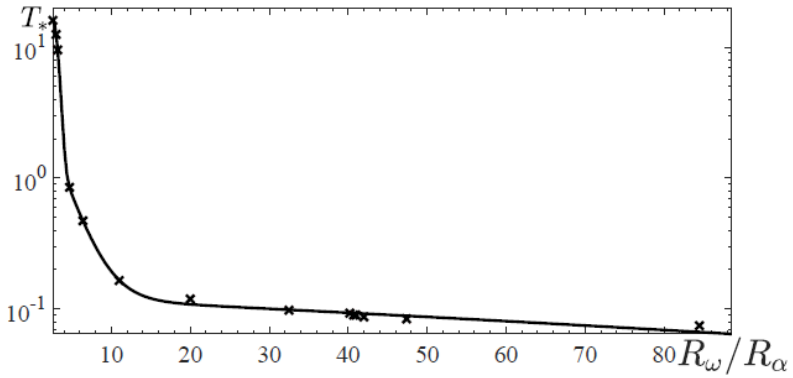

Figure 10. The period T_* of the stellar magnetic cycles normalized by 122.2 years versus R_ω/R_α obtained from numerical simulations of the non-linear $\alpha^2\Omega$ mean-field dynamo.

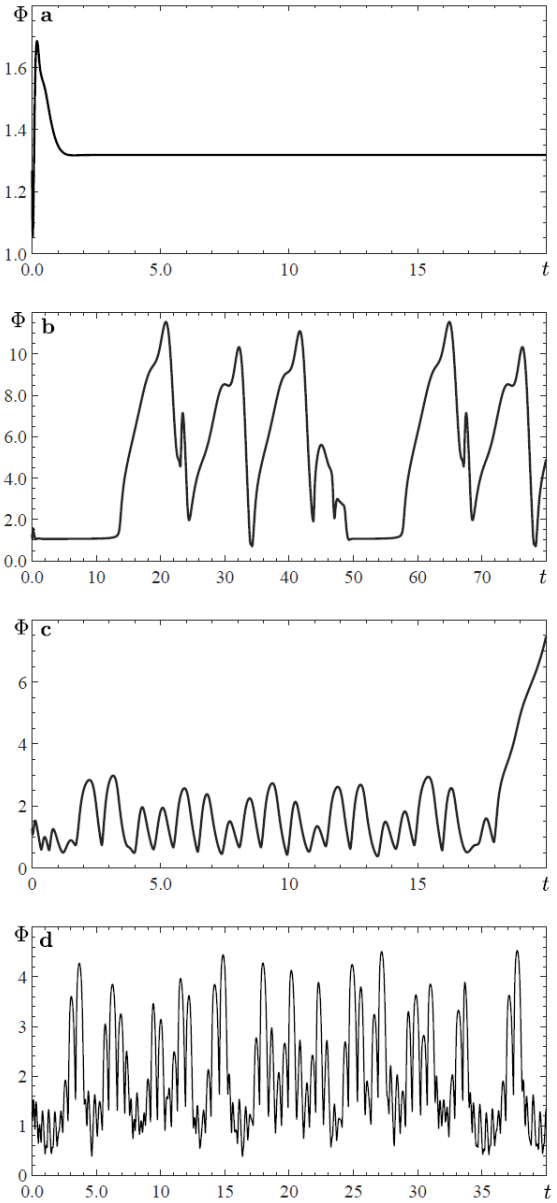

Figure 9. The time evolution of the flux of the toroidal mean magnetic field $\Phi = \int |\overline{B}_\varphi|\, d\sigma$ obtained from numerical simulations of $\alpha^2\Omega$ mean-field dynamo at different values of $R_\omega/R_\alpha =$ 1.6 (**a**); 3.2 (**b**); 4.7 (**c**) and 6.4 (**d**). The time is normalized by 122.2 years, and the flux Φ is normalized by the magnetic field of 300 G.

Threshold for the Stellar Dynamos

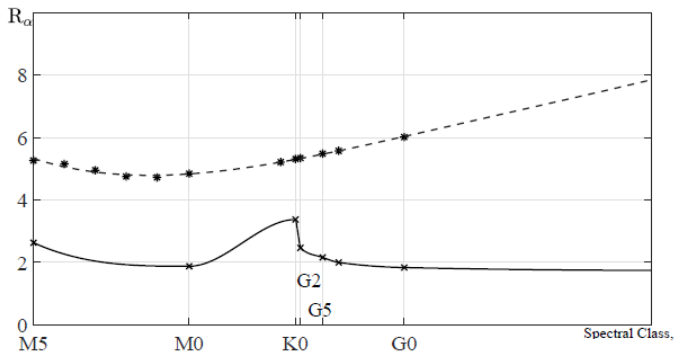

Figure 12. The threshold $R_\alpha^{\rm cr}$ (snowflakes, dashed line) in generation of the large-scale magnetic field and the parameter R_α (crosses, solid line) versus the parameter μ obtained from numerical simulations of the non-linear α^2 mean-field dynamo. The parameter $R_\alpha = (\Omega_\odot/\eta_T)^{1/2} R_*$ is determined for the main sequence stars, where the angular velocity coincides with the mean (averaged over the latitude) solar angular velocity $\Omega_\odot$.

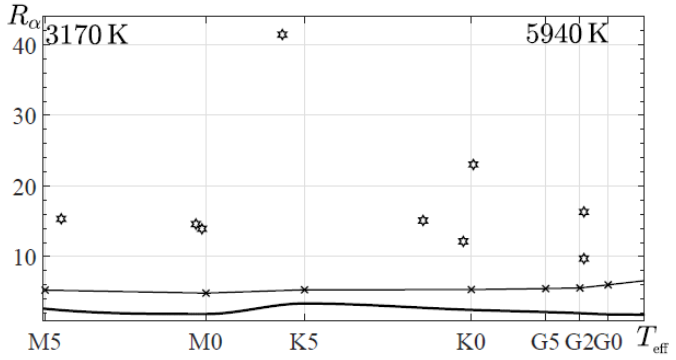

Figure 13. The threshold $R_\alpha^{\rm cr}$ (crosses, thin solid line) in generation of the large-scale magnetic field and the parameter $R_\alpha = (\Omega_\odot/\eta_T)^{1/2} R_*$ (solid line) versus the star effective temperature $T_{\rm eff}$ obtained from numerical simulations of the non-linear α^2 mean-field dynamo. The parameter R_α is calculated for the main sequence stars, where the angular velocity coincides with the mean (averaged over the latitude) solar angular velocity $\Omega_\odot$. The parameter $\tilde{R}_\alpha$ (stars) is also estimated for real main sequence stars, where we use equation (5), the rotating rates (see Gershberg et al. 2021) and turbulent magnetic diffusion coefficients for the stars of these spectral classes.

$$\alpha_* = C_*(\Omega_* \eta_{\rm T})^{1/2},$$

Table 1. The coefficient C_* for different spectral classes and different rotation rates.

spectral class	$\Omega_\odot$	$10\Omega_\odot$	$20\Omega_\odot$
G2	0.970	0.933	0.982
K2	0.877	0.874	0.883
K4	0.824	0.858	0.854
K7	0.855	0.815	0.793
M2	0.643	0.687	0.680

The magnetic field of fast rotating stars cannot be explained by pure α^2 dynamo, because some observed features (appearance of star spots in the polar regions, long period of cyclic behaviour, etc.) for the main sequence fast rotating stars require presence of small differential rotation.

Stellar Dynamos

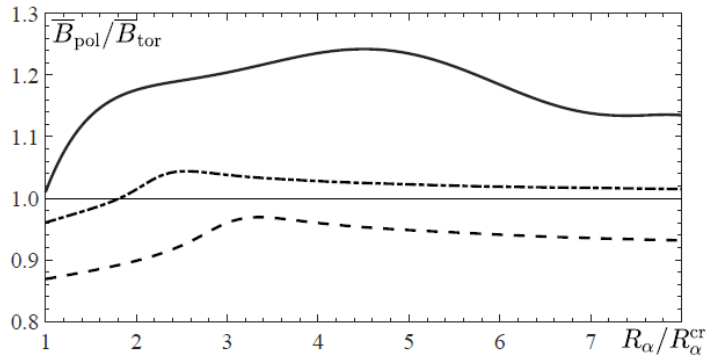

Figure 14. The ratio of the maximum values of the poloidal to toroidal mean magnetic fields $\overline{B}_{\rm pol}/\overline{B}_{\rm tor}$ versus $R_\alpha/R_\alpha^{\rm cr}$ for the main sequence stars of three spectral classes: M5 (solid); M0 (dashed-dotted); K5 (dashed), obtained from numerical simulations of the non-linear α^2 mean-field dynamo.

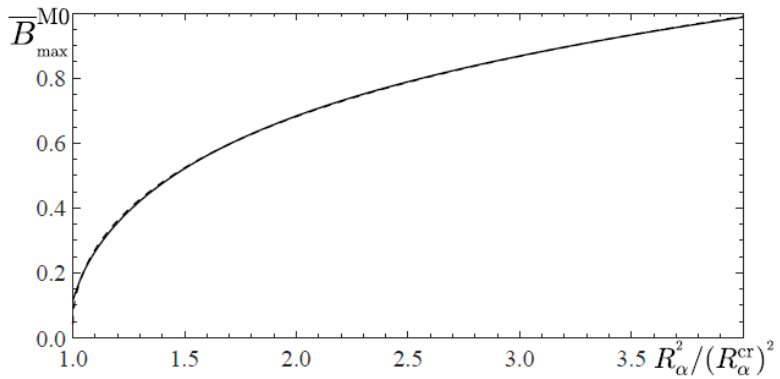

Figure 15. The maximum mean magnetic field $\overline{B}_{\rm max}^{\rm M0}$ versus $(R_\alpha^2/R_\alpha^{\rm cr})^2$ for the main sequence stars of the spectral class M0, obtained from numerical simulations (solid) of the non-linear α^2 mean-field dynamo and analytical result (dashed) described by equations (38) and (39).

$$\overline{B} = (2\pi\overline{\rho}_*)^{1/2}\ \frac{3\eta_T\,\kappa_T}{R_*}\ \left(\frac{2GT_\alpha}{K}\right)^{1/2}\ f\left[\frac{R_\alpha^2}{(R_\alpha^{\rm cr})^2}\right],$$

$$f(X) = \left(\frac{X-1}{X-C}\right)^{1/2}\ \left[(R_\alpha^{\rm cr})^2 X + 2\right]^{-1}$$
$$\times\left[1 - 2G\,\frac{(R_\alpha^{\rm cr})^2 X(X-1)}{(X-C)\,\left[(R_\alpha^{\rm cr})^2 X + 2\right]}\,\frac{\overline{\boldsymbol{b}}_p^2}{t_\chi}\right.$$
$$\left.+\left(1 - 4G\,\frac{(R_\alpha^{\rm cr})^2 X(X-1)}{(X-C)\,\left[(R_\alpha^{\rm cr})^2 X + 2\right]}\,\frac{\overline{\boldsymbol{b}}_p^2}{t_\chi}\right)^{1/2}\right]^{-1/2}$$

Previous Mean-Field Studies

- Various mean-field dynamo models have been suggested to explain generation of large-scale magnetic fields in M dwarfs (Chabrier and Kuker 2006; Kitchatinov, Moss and Sokoloff 2014; Shulyak et al. 2015; Pipin 2017; Pipin and Yokoi 2018).

- Mean-field simulations (MFS) of the kinematic α^2 dynamo have been performed by Chabrier and Kuker (2006). They found that the dynamo generates a non-axisymmetric steady magnetic field that is symmetric with respect to the equatorial plane.

- Kitchatinov et al. (2014) used a kinematic model of an $\alpha^2\Omega$ dynamo with the differential rotation determined using the numerical mean-field model by Kitchatinov and Olemskoy (2011). They suggested that M-dwarfs have two types of magnetic activity: (i) magnetic cycles with strong (kilogauss) almost axisymmetric poloidal magnetic fields; and (ii) considerably weaker non-axisymmetric fields with a substantial toroidal component observed at times of magnetic field inversion.

- Pipin (2017) performed MFS of the non-linear axisymmetric and non-axisymmetric dynamos of the fully convective star using the model of differential rotation by Kitchatinov and Olemskoy (2011). The dynamical quenching of the alpha effect is described by equation for the total magnetic helicity density.

Summary

- Our theoretical and numerical analysis have suggested that for low-mass main sequences stars (of the spectral classes from M5 to G2) rotating much faster than the Sun, the generated large-scale magnetic field is caused by the mean-field $\alpha^2\Omega$ dynamo, whereby the α^2 dynamo is modified by a weak differential rotation.
- Even for a weak differential rotation, the behaviour of the magnetic activity is changed drastically from aperiodic regime to non-linear oscillations and appearance of a chaotic behaviour with increase of the differential rotation.
- Periods of the magnetic cycles decrease with increase of the differential rotation, and they vary from tens to thousand years. This long-term behaviour of the magnetic cycles may be related to the characteristic time of the evolution of the magnetic helicity density of the small-scale field.
- The performed analysis is based on the mean-field simulations (MFS) of the $\alpha^2\Omega$ and α^2 dynamos and a developed non-linear theory of the dynamos.

THE END